

Autophagy suppresses resveratrol-induced apoptosis in renal cell carcinoma 786-O cells

HONGWEI YAO, MIN FAN and XIAOZHOU HE

Department of Urology, The Third Affiliated Hospital of Soochow University, Changzhou, Jiangsu 213003, P.R. China

Received April 10, 2019; Accepted November 12, 2019

DOI: 10.3892/ol.2020.11442

Abstract. As a polyphenolic compound, resveratrol (Res) is widely distributed in a variety of plants. Previous studies have demonstrated that Res can inhibit various different types of tumor growth. However, its role in renal cell carcinoma (RCC) remains largely unknown. The present study first demonstrated that Res inhibited cell viability and induced apoptosis in RCC 786-O cells. Further experiments revealed that Res damaged the mitochondria and activated caspase 3. In contrast, Z-VAD-FMK, a pan-caspase inhibitor, suppressed Res-induced apoptosis. Reactive oxygen species (ROS) were involved in the process of Res-induced apoptosis, and antioxidant N-acetyl cysteine could significantly attenuate this. Furthermore, Res activated c-Jun N-terminal kinase via ROS to induce autophagy, whereas inhibition of autophagy with chloroquine or Beclin 1 small interfering RNA aggravated Res-induced apoptosis, indicating that autophagy served as a pro-survival mechanism to protect 786-O cells from Res-induced apoptosis. Therefore, a combination of Res and autophagy inhibitors could enhance the inhibitory effect of Res on RCC.

Introduction

Renal cell carcinoma (RCC) is the most common subtype of kidney cancer that accounts for 3% of all malignancies in adults in the United States (1). RCC incidence rates among men in 2012 varied from ~1 in Africa to >15 in Europe (cases per 100,000 standard population) (2). RCC is resistant to radiotherapy and chemotherapy, and surgical resection remains the primary therapeutic technique for early-localized RCC. Between 25-30% of patients have metastatic disease at the time of RCC diagnosis, and patients with metastatic RCC have a very poor prognosis (3). Although a great deal of progress

has been made in targeted molecular therapy for the treatment of metastatic RCC, their medicinal performance remains less than satisfactory.

Resveratrol (Res), a polyphenolic compound, is widely distributed in a variety of plants (4). Since the first study reported its inhibitory effect on carcinogenesis in a mouse skin cancer model in 1997 (5), a large number of studies have demonstrated that Res can inhibit multiple types of cancer *in vitro*. Furthermore, Res also possesses antitumor effects *in vivo* (6). However, the antitumor effect of Res on RCC remains largely unknown due to its complex pharmacological activities. The present study aimed to investigate the underlying molecular mechanism of Res in RCC.

The 786-O cell line possesses numerous characteristics of RCC, including mutations in the VHL gene (7) and high activation of vascular endothelial growth factor (VEGF) (8), and is widely used in RCC research. The present study revealed that in 786-O cells, Res damaged mitochondria, activated caspase 3 and induced apoptosis through reactive oxygen species (ROS). Furthermore, Res activated c-Jun N-terminal kinase (JNK) via ROS to induce autophagy, while inhibition of autophagy further exacerbated Res-induced apoptosis.

Materials and methods

Reagents and antibodies. Res was purchased from Selleck Chemicals. A Cell Counting Kit-8 (CCK-8) was obtained from Dojindo Molecular Technologies, Inc. Z-VAD-FMK was purchased from Santa Cruz Biotechnology, Inc. Chloroquine (CQ) was supplied by Enzo Life Sciences, Inc. N-acetyl cysteine (NAC) and 2',7'-dichlorofluorescein-diacetate (DCFH-DA) were purchased from Beyotime Institute of Biotechnology. SB203580 and SP600125 were obtained from MedChemExpress. Antibodies against PARP (1:1,000; catalog no. 9532), GAPDH (1:2,000; catalog no. 5714), AMPK α (1:1,000; catalog no. 5831), p-AMPK α (1:1,000; catalog no. 2535), S6 (1:1,000; catalog no. 2317), p-S6 (1:1,000; catalog no. 4858), p38 (1:1,000; catalog no. 8690), p-p38 (1:1,000; catalog no. 4511), JNK (1:1,000; catalog no. 9252), p-JNK (1:1,000; catalog no. 4668), ERK (1:1,000; catalog no. 4695), p-ERK (1:1,000; catalog no. 4370), BCL2 (1:1,000; catalog no. 4223) and p-BCL2 (1:1,000; catalog no. 2827) were all purchased from Cell Signaling Technology, Inc. LC3B antibody (1:1,000; catalog no. ab192890) was purchased from

Correspondence to: Dr Xiaozhou He, Department of Urology, The Third Affiliated Hospital of Soochow University, 185 Juqian Street, Changzhou, Jiangsu 213003, P.R. China
E-mail: fnmong@hotmail.com

Key words: resveratrol, apoptosis, reactive oxygen species, autophagy

Abcam, and Beclin 1 antibody (1:500; catalog no. sc-48341) was purchased from Santa Cruz Biotechnology, Inc.

Cell culture. The 786-O cell line was purchased from the Shanghai Institute of Cell Biology, Chinese Academy of Sciences. Cells were maintained in RPMI-1640 medium (HyClone; GE Healthcare Life Sciences) supplemented with 10% FBS (Gibco; Thermo Fisher Scientific, Inc.) and 1% penicillin and streptomycin, at 37°C in a humidified atmosphere containing 5% CO₂ until they reached 80-90% confluence.

Cell viability assay. Cell viability assay was performed using CCK-8 reagent (Dojindo Molecular Technologies), according to the manufacturer's protocol. The 786-O cells were seeded at a density of 4x10³ cells/well into 96-well plates. Following overnight incubation at 37°C, the cells were treated with the indicated concentrations of Res (10, 20, 40 and 80 μM) for 24 or 48 h. Following Res treatment, CCK-8 reagent was added into every well, followed by incubation at 37°C for 1 h in the dark. Subsequently, the optical density was determined using a microplate reader (Bio-Rad Laboratories, Inc.), at a wavelength of 450 nm.

Cell apoptosis assay. Cell apoptosis was assessed using an AnnexinV-FITC-propidium iodide (PI) double staining kit (MultiSciences Biotech, Co., Ltd.), according to the manufacturer's protocol. Briefly, cells were treated with 10, 20 μM Res for 48, and 40 μM of Res for 24 or 48 h. For some experiments, cells were treated with 40 μM Res for 48 h in the presence or absence of 50 μM Z-VAD-FMK, 10 mM NAC or 50 μM CQ. Following treatment, cells were harvested and washed twice with PBS. Subsequently, cells were incubated in buffer containing Annexin V-FITC and PI at room temperature for 5 min in the dark. Apoptotic cells were identified using a BD FACSCanto II flow cytometer (BD Biosciences) and data were analyzed using FACSDiVa software (version 7.0; BD Biosciences).

ROS assay. Cells were harvested, washed twice with PBS, and then incubated in serum-free RPMI-1640 medium containing DCFH-DA at 37°C for 20 min. Cells were re-washed twice with PBS and intracellular ROS was detected via the aforementioned flow cytometry method.

Caspase 3 activity assay. Caspase 3 activity was determined using a caspase 3 activity assay kit (ApexBio Technology), according to the manufacturer's protocol. Briefly, cells were washed twice with PBS and incubated in staining buffer containing FITC-DEVD-FMK probe at 37°C for 30 min. Cells were re-washed twice with PBS and harvested, and caspase 3 activity was detected via the aforementioned flow cytometry method.

Mitochondrial membrane potential ($\Delta\Psi_m$) assay. The $\Delta\Psi_m$ assay was performed using a JC1 mitochondrial membrane potential assay kit (Beijing Solarbio Science & Technology Co., Ltd.), according to the manufacturer's protocol. In brief, cells were washed twice with PBS and incubated in fresh RPMI-1640 medium containing JC1 reagent at 37°C for 30 min.

Cells were re-washed twice with PBS and harvested, and $\Delta\Psi_m$ was determined via the aforementioned flow cytometry method. $\Delta\Psi_m$ was calculated as the ratio of red to green fluorescence.

Cyto-ID autophagy detection assay. A CYTO-ID autophagy detection kit (Enzo Life Sciences, Inc.) was utilized in the present study. Briefly, cells were washed twice with PBS and then incubated in PBS containing CYTO-ID probe and 5% FBS at 37°C for 20 min in the dark. Following the incubation, cells were re-washed twice with PBS and observed under a fluorescence microscope (Olympus Corporation; magnification, x200). In order to evaluate autophagy with flow cytometry, cells were harvested following incubation with CYTO-ID probe at 37°C for 20 min in the dark. Subsequently, autophagy was determined via the aforementioned flow cytometry method.

Western blotting. Cells were treated with 40 μM Res for 24 or 48 h. For some experiments, 10 mM NAC, 20 μM SP600125 or 20 μM SB203580 were used. In order to evaluate autophagic flux, cells were treated with 40 μM Res for 48 h in the presence or absence of 50 μM CQ.

Cells were lysed using a total protein extraction kit (Nanjing KeyGen Biotech Co., Ltd.), according to the manufacturer's protocol. Protein concentrations were determined using a bicinchoninic acid assay kit (Nanjing KeyGen Biotech Co., Ltd.) and 30 μg protein/lane was separated via SDS-PAGE on a 10-12% gel. The separated proteins were subsequently transferred onto a polyvinylidene difluoride membrane and blocked with 5% BSA 1 h at room temperature. The membranes were incubated with the aforementioned primary antibodies, overnight at 4°C. The membranes were then washed three times with TBST and incubated with corresponding anti-rabbit or anti-mouse HRP-conjugated secondary antibodies (1:5,000; catalog no. GAR007 and GAM007; MultiSciences Biotech, Co., Ltd.) at room temperature for 1 h. Protein bands were visualized using an ECL system (EMD Millipore) and densitometric analysis was performed using ImageJ software (version 1.48v; National Institutes of Health).

Small interfering (si)RNA and transfection. Beclin 1 (catalog no. sc-29797) and scrambled control siRNA (catalog no. sc-37007) were purchased from Santa Cruz Biotechnology, Inc. The Beclin 1 siRNA sequences were as follows: Forward, 5'-CAGCUCAACGUCACUGAAATT-3' and reverse, 5'-UUU CAGUGACGUUGAGCUGTT-3'. The control siRNA sequences were not available. Briefly, 100 nM of Beclin 1 or control siRNA was transfected into cells using Lipofectamine® 2000 reagent (Invitrogen; Thermo Fisher Scientific, Inc.), according to the manufacturer's protocol, and non-transfected cells were set as a blank control. After 24 h, cells were treated with 40 μM Res for an additional 48 h and subsequently analyzed via western blotting as previously described.

Statistical analysis. All experiments were performed in triplicate, and the data are presented as the mean ± standard deviation. Unpaired Student's t-test was used for comparisons between two groups. One-way analysis of variance followed by post hoc comparisons using Tukey's test was used for

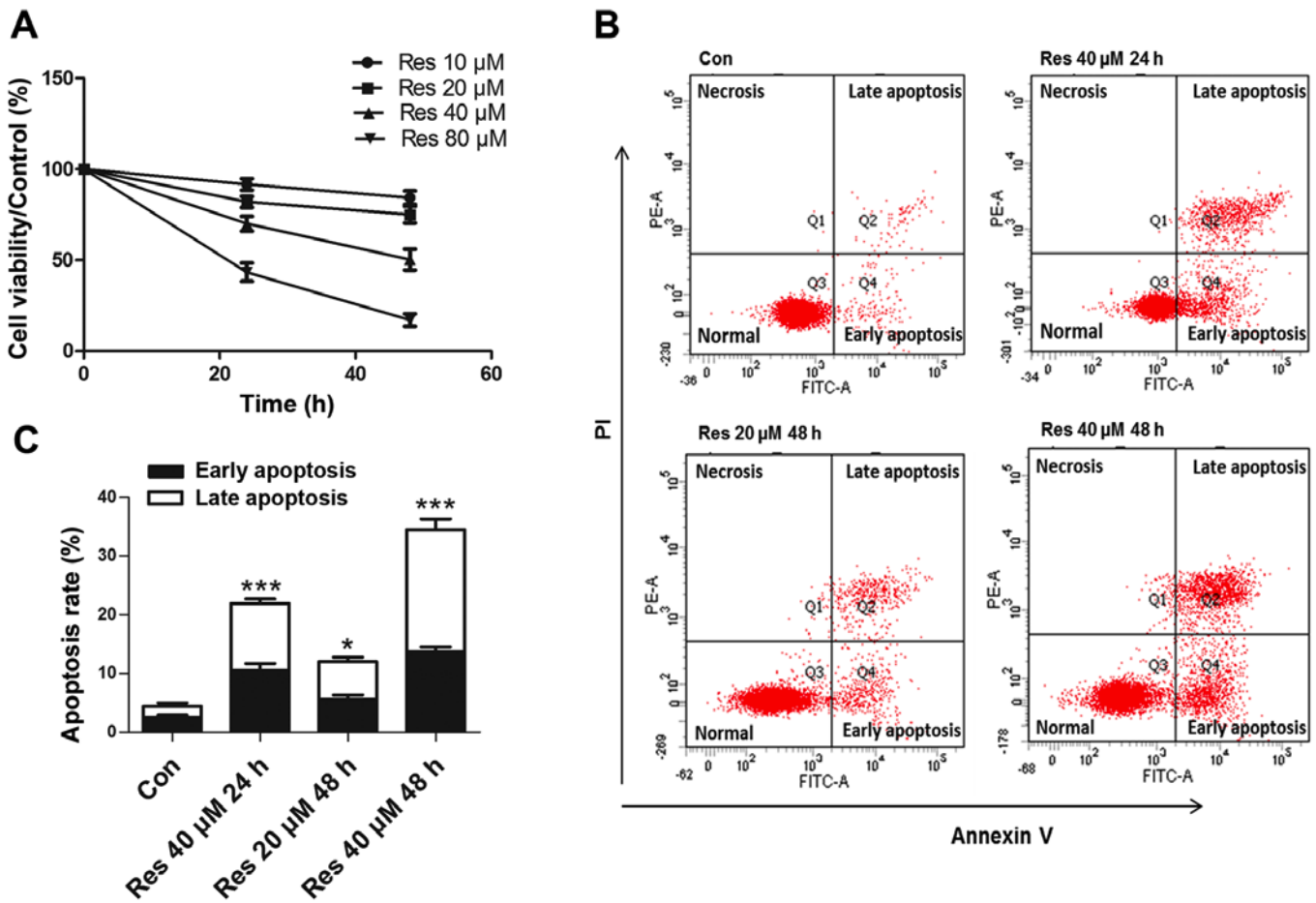


Figure 1. Res decreases cell viability and induces apoptosis in 786-O cells. (A) Cell viability was analyzed using a Cell Counting Kit-8 assay. (B) Representative images of the flow cytometric apoptosis assay. (C) Quantitative analysis of apoptosis detected by flow cytometry. *P<0.05, ***P<0.001 vs. control group. Res, resveratrol.

comparisons between three groups or more. P<0.05 was considered to indicate a statistically significant difference.

Results

Res inhibits cell viability and induces apoptosis of 786-O cells. The 786-O cells were exposed to various concentrations of Res (10, 20, 40 and 80 μM) for 24 and 48 h. The CCK-8 assay revealed that Res inhibited the cell viability in a time- and dose-dependent manner (Fig. 1A). Since a previous study (9) reported that high concentrations (≥50 μM) of Res exhibited significant toxicity to normal renal epithelial cells, the present study performed further experiments at lower concentrations. The flow cytometric analysis revealed that Res at 20 and 40 μM induced apoptosis (Fig. 1B and C), while 10 μM Res had no effect on apoptosis (data not shown).

Res damages mitochondria and activates caspase to induce apoptosis. Mitochondria are the key elements for apoptotic execution, and damaged mitochondria can release pro-apoptotic factors that activate caspase to induce apoptosis. ΔΨm is an important parameter in the evaluation of mitochondrial function (10). The present study observed that Res decreased ΔΨm (Fig. 2A and B), activated caspase 3 (Fig. 2C), and induced cleavage of PARP, a substrate of caspase 3 (Fig. 2D).

Furthermore, Z-VAD-FMK, a pan-caspase inhibitor, significantly inhibited apoptosis (Fig. 2E), demonstrating that Res induced apoptosis in 786-O cells primarily through the activation of caspase.

ROS is responsible for Res-induced apoptosis. As an important signaling factor, normal ROS levels can maintain cell homeostasis, while excessive ROS can cause cell injury (11). Res significantly increased the ROS level in 786-O cells (Fig. 3A and B). NAC, an antioxidant, attenuated ROS production (Fig. 3C), improved ΔΨm (Fig. 3D), decreased caspase 3 activity (Fig. 3E), impaired apoptosis (Fig. 3F) and decreased the cleavage of PARP (Fig. 3G), suggesting that Res could damage mitochondria, activate caspase 3 and cause apoptosis through ROS in 786-O cells.

Res induces autophagy partially through ROS. As a conservative mechanism, autophagy can be activated in multiple environments, including nutritional deficiency, hormone imbalance and oxidative stress, among others (12). The Cyto-ID fluorescent probe specifically labels autophagosomes in live cells (13), which was used to assess whether Res initiated autophagy in the present study. The results revealed that Res stimulated the formation of autophagosomes in 786-O cells (Fig. 4A), and the flow cytometric assay

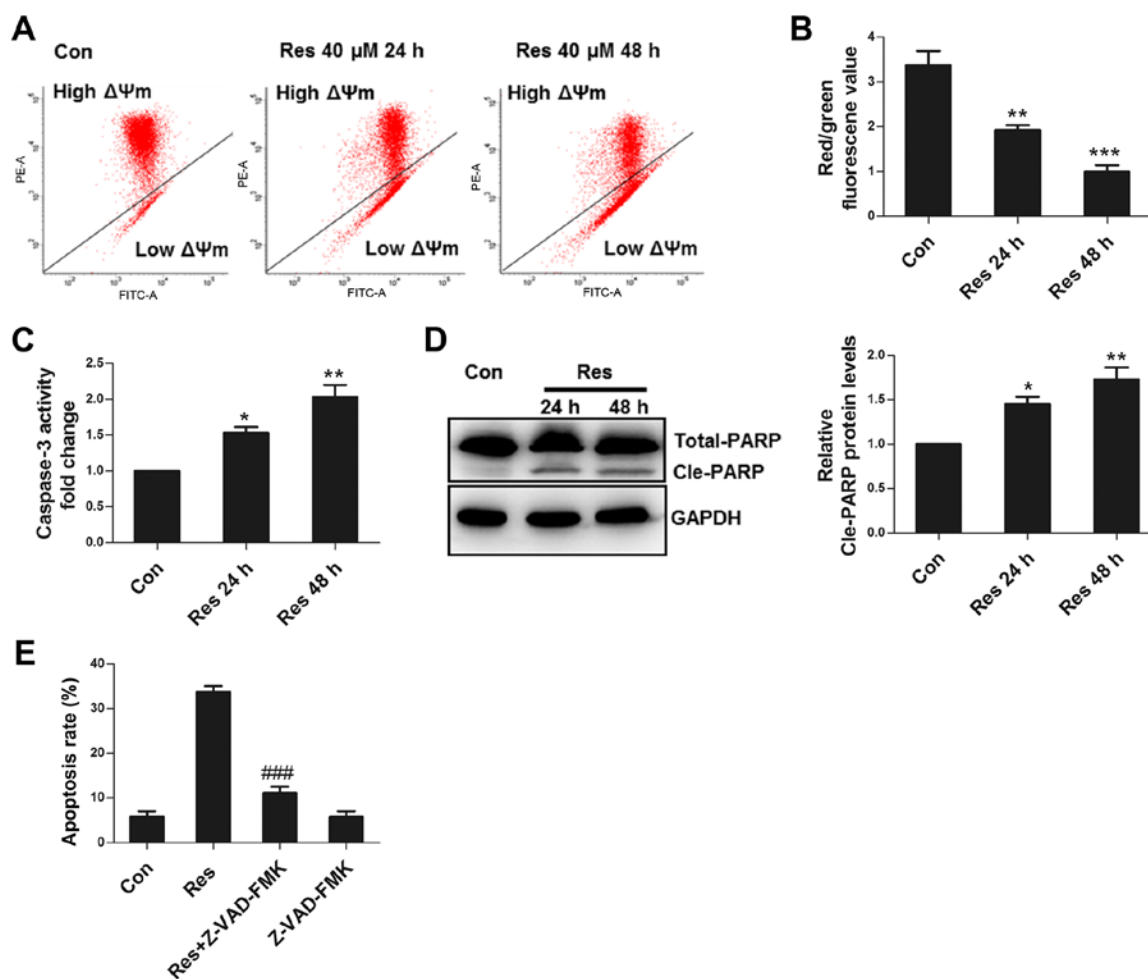


Figure 2. Res damages mitochondria and activates caspase to execute apoptosis. (A) Representative images of flow cytometric assay for $\Delta\Psi_m$. (B) Quantitative analysis of JC1 red/green fluorescence value as detected by flow cytometry. (C) Quantitative analysis of caspase 3 activity detected by flow cytometry. (D) Following treatment with 40 μM Res for 24 or 48 h, a western blot analysis to detect changes in PARP was performed. (E) Following treatment with 40 μM Res in the presence or absence of 50 μM Z-VAD-FMK for 48 h, quantitative analysis of apoptosis detected by flow cytometry was performed. * $P < 0.05$, ** $P < 0.01$, *** $P < 0.001$ vs. control group; ### $P < 0.001$ vs. Res group. Res, resveratrol; $\Delta\Psi_m$, mitochondrial membrane potential.

further confirmed these findings (Fig. 4B). Furthermore, Res increased the expression level of autophagy marker protein LC3B II (Fig. 4C). Since the upregulation of LC3B II can reflect activated autophagy or impaired autophagic flux, the present study inhibited the degradation of autophagy using autophagy inhibitor CQ, which further upregulated the expression of LC3B II at the protein level (Fig. 4D), indicating that Res induced complete autophagic flux. ROS has been well known as a signaling molecule regulating autophagy (14); therefore, the present study subsequently assessed whether ROS participated in Res-induced autophagy in 786-O cells. As expected, inhibition of ROS by NAC attenuated the expression of LC3B II (Fig. 4E), suggesting that Res induced autophagy partially through ROS.

JNK activated by ROS is required for Res-induced autophagy. ROS can induce autophagy through multiple signaling pathways, including AMPK-mammalian target of rapamycin (mTOR) (15), p53 (16) and MAPK (17). Since the status of p53 remains controversial in 786-O cells (18), the present study did not investigate its role here. Res had no effect on the expression levels of p-AMPK and p-S6 protein, a downstream

protein in the mTOR signaling pathway (Fig. 5A), indicating that the AMPK-mTOR signaling pathway was not involved in the autophagic process in the experiments performed in the present study. The present study further investigated the MAPK family-associated proteins (ERK, JNK and p38) and revealed that Res inhibited ERK, and activated JNK and p38 (Fig. 5B). Notably, NAC reversed the effects of Res on ERK, JNK and p38 (Fig. 5C). SB203580 (a p38 inhibitor) increased the expression of LC3B II, while in contrast, SP600125 (a JNK inhibitor) attenuated the expression of LC3B II (Fig. 5D), suggesting that Res activated JNK via ROS to induce autophagy. JNK phosphorylates the BCL2 protein, resulting in the dissociation of Beclin 1 from BCL2 to activate autophagy (19). Indeed, it was revealed in the present study that SP600125 decreased the Res-induced upregulation of phosphorylated BCL2 in 786-O cells (Fig. 5E).

Inhibition of autophagy enhances Res-induced apoptosis. Since autophagy can promote cell survival or death in different environments (20), the present study used CQ to inhibit autophagy and it was observed that CQ exacerbated Res-induced apoptosis in 786-O cells (Fig. 6A). In addition,

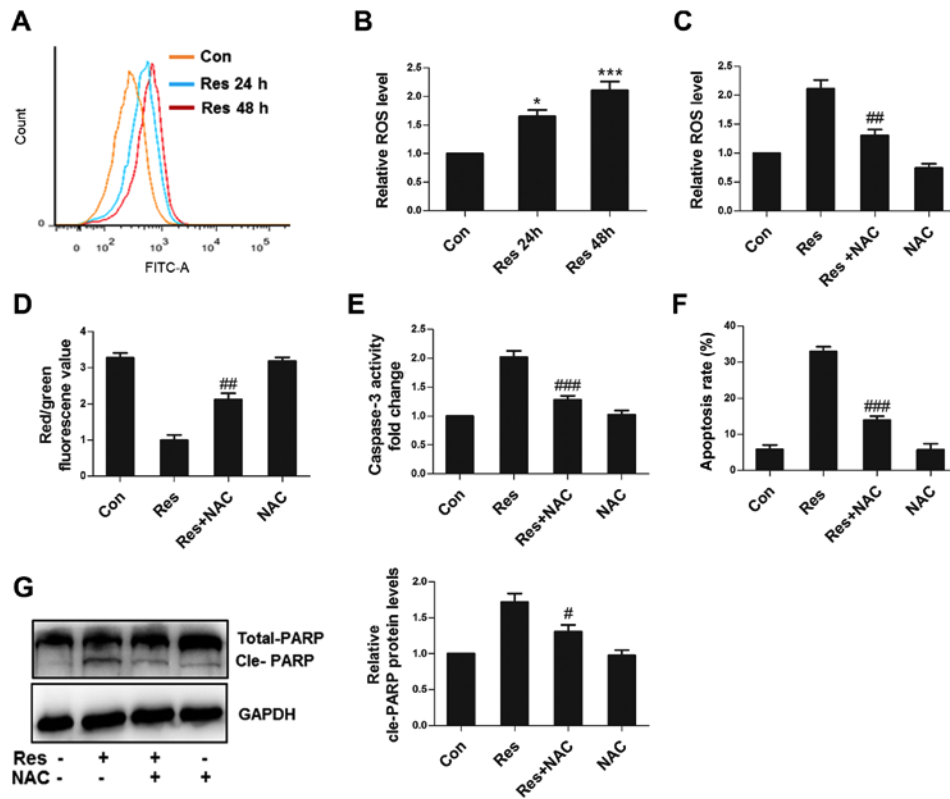


Figure 3. ROS are responsible for apoptosis induced by Res. (A) Following treatment with 40 μ M Res for 24 or 48 h, representative images of flow cytometric assay for ROS. (B) Following treatment with 40 μ M Res for 24 or 48 h, quantitative analysis of ROS detected by flow cytometry was performed. Following treatment with 40 μ M Res in the presence or absence of 10 mM NAC for 48 h, quantitative analysis of (C) ROS, (D) JC1 red/green fluorescence value, (E) caspase 3 activity, (F) apoptosis and (G) western blot analysis of PARP expression were detected by flow cytometry. * P <0.05, *** P <0.001 vs. control group; # P <0.05, ## P <0.01, ### P <0.001 vs. Res group. ROS, reactive oxygen species; Res, resveratrol; NAC, N-acetyl cysteine.

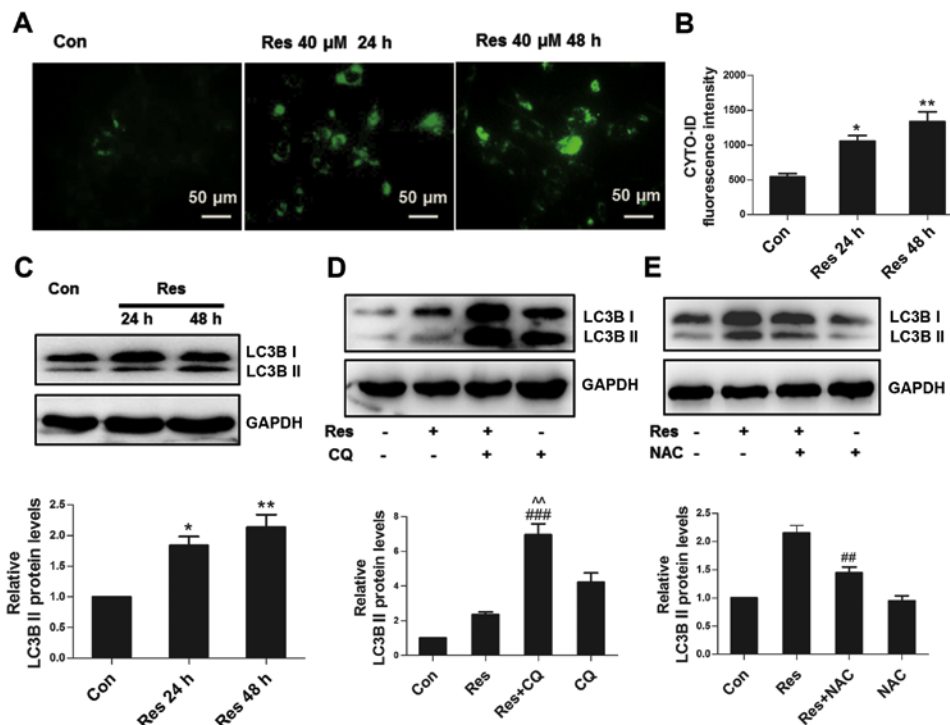


Figure 4. Res induces autophagy partially through ROS. (A) Representative Cyto-ID fluorescence assay images by fluorescence microscope. (B) Quantitative analysis of Cyto-ID fluorescence detected by flow cytometry. (C) Following treatment with 40 μ M Res for 24 h or 48 h, western blot analysis of LC3B was performed. (D) Following treatment with 40 μ M Res in the presence or absence of 50 μ M CQ for 48 h, western blot analysis of LC3B was performed. (E) Following treatment with 40 μ M Res in the presence or absence of 10 mM NAC for 48 h, western blot analysis of LC3B was performed. * P <0.05, ** P <0.01 vs. control group; # P <0.001, ### P <0.001 vs. Res group. ** P <0.01 vs. CQ group. Res, resveratrol; ROS, reactive oxygen species; CQ, chloroquine; NAC, N-acetyl cysteine.

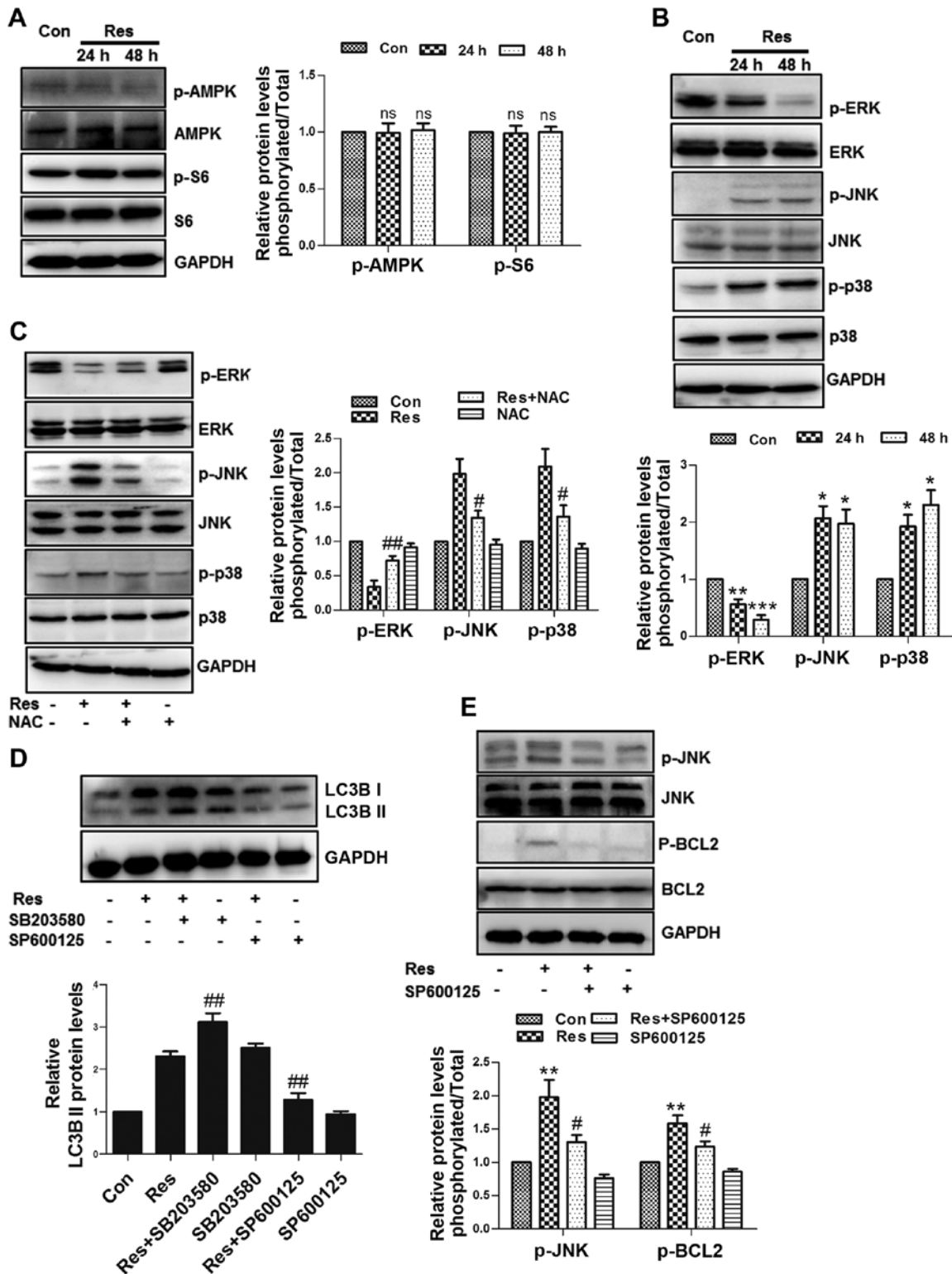


Figure 5. JNK activated by ROS is required for Res-induced autophagy. Following treatment with 40 μ M Res for 24 h or 48 h, (A) western blot analysis of p-AMPK and p-S6, and (B) p-ERK, p-p38, p-JNK, ERK, p38 and JNK was performed. (C) Following treatment with 40 μ M Res in the presence or absence of 10 mM NAC for 48 h, western blot analysis of p-ERK, p-p38 and p-JNK was performed. (D) Following treatment with 40 μ M Res in the presence of 20 μ M SB203580 or 20 μ M SP600125 for 48 h, western blot analysis of LC3B was performed. (E) Following treatment with 40 μ M Res in the presence or absence of 20 μ M SP600125 for 48 h, western blot analysis of p-JNK and p-BCL2. NS, *P<0.05, **P<0.01, ***P<0.001 vs. control group; #P<0.05, ##P<0.01 vs. Res group. JNK, c-Jun N-terminal kinase; ROS, reactive oxygen species; Res, resveratrol; NAC, N-acetyl cysteine; NS, not significant.

CQ further activated caspase 3 (Fig. 6B) and promoted the cleavage of PARP (Fig. 6C). However, CQ alone did not affect the amount of apoptosis, caspase 3 activity and cleavage of PARP. Beclin 1, a conserved protein, initiates autophagosome

formation, thus playing a central role during the autophagic process (21). siRNA-mediated Beclin 1 knockdown increased the level of cleaved PARP (Fig. 6D), further confirming that autophagy could suppress Res-induced apoptosis in 786-O cells.

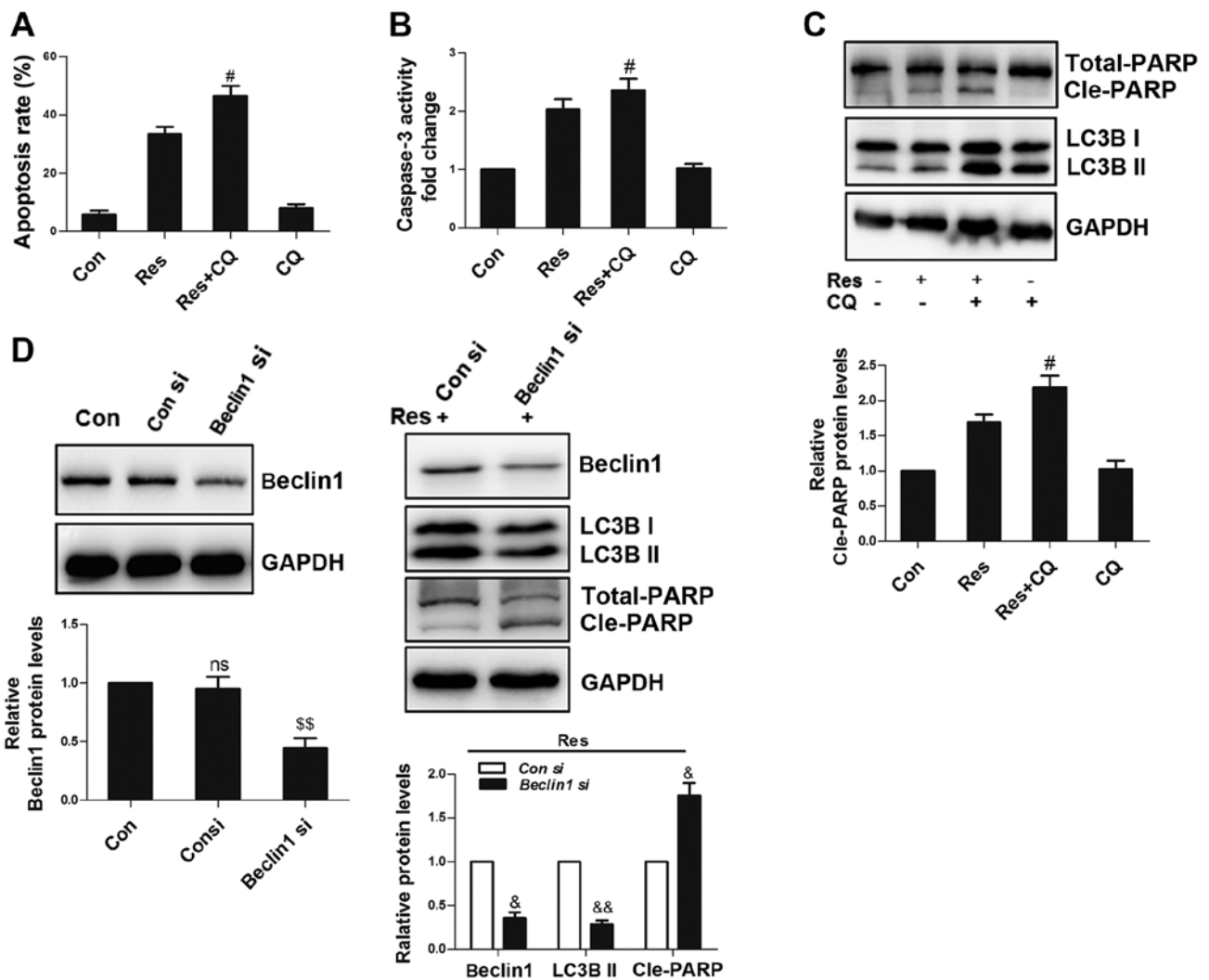


Figure 6. Inhibition of autophagy enhances Res-induced apoptosis. Following treatment with 40 μ M Res in the presence or absence of 50 μ M CQ for 48 h, quantitative analysis of (A) apoptosis and (B) caspase 3 activity were detected by flow cytometry, and (C) via western blot analysis of PARP and LC3B. (D) Cells were transfected with 100 nM Beclin 1 siRNA or control siRNA, and non-transfected cells were set as a blank control. After 24 h, cells were treated with 40 μ M Res for an additional 48 h, and western blotting was used for the analysis of Beclin 1, LC3B and PARP expressions. NS vs. control group; [#]P<0.05 vs. Res group; ^{\$\$}P<0.01 vs. con siRNA group; [&]P<0.05, ^{&&}P<0.01 vs. con siRNA+Res group. NS, not significant; Res, resveratrol; CQ, chloroquine; siRNA, small interfering RNA.

Discussion

Mitochondria play an important role in the process of cell death. Damaged mitochondria can release cytochrome c to activate caspase 3 for the execution of apoptosis, or translocate apoptosis-inducing factor into the nucleus, leading to caspase-independent apoptosis (22). $\Delta\Psi_m$ disruption is a key event in apoptosis (23). It was observed in the present study that Res decreased the $\Delta\Psi_m$, activated caspase 3 and caused the cleavage of PARP. Furthermore, caspase inhibitor Z-VAD-FMK significantly inhibited Res-induced apoptosis. All the aforementioned findings suggested that Res induced apoptosis via mitochondria in a caspase-dependent manner in 786-O cells.

Res acts as an antioxidant or pro-oxidant depending on the environment and cell type (24). Previous studies have demonstrated that Res causes tumor cell death through ROS (25,26), and that Res promotes the production of ROS in 786-O cells (27). However, the authors did not investigate the association between ROS and cell death further. Indeed, in certain circumstances,

elevated ROS is only an event that accompanies cell death, and even enhanced ROS production can play a protective role in decreasing the amount of cell death (28,29). The present study clearly revealed that inhibition of ROS by NAC significantly attenuated apoptosis, suggesting that ROS was responsible for Res-induced apoptosis in 786-O cells.

Previous studies have demonstrated that Res can activate (30,31) or inhibit autophagy (32,33). The present study confirmed that Res activated autophagy and induced complete autophagic flux in 786-O cells. Furthermore, Res induced autophagy partially through ROS. AMPK-mTOR is a classic regulatory signaling pathway in autophagy (34). However, in the experiments performed in the present study, Res did not affect AMPK and mTOR, indicating that Res induced non-classical autophagy. Previous research has reported that p38 inhibits autophagy (35) and that JNK can promote autophagy by phosphorylating BCL2 (19). The present study revealed that Res activated JNK and p38 through ROS, while inhibition of p38 or JNK promoted or attenuated autophagy, respectively. Furthermore, inhibition of JNK decreased the

increased amount of BCL2 phosphorylation, suggesting that JNK was involved in the autophagic process. It was also noted that Res inhibited ERK activity. ERK can activate HIF-1 α to promote VEGF transcription (36). Notably, high expression of VEGF is a common feature of RCC, and the association between Res and ERK deserves further investigation.

Under oxidative stress, the association between autophagy and apoptosis is complicated. On the one hand, autophagy can capture damaged proteins and organs (such as damaged mitochondria) for degradation, maintaining cell survival. On the other hand, extreme autophagy promotes cell death (37). In the experiments performed in the present study, autophagy inhibitor CQ and Beclin 1 siRNA further promoted apoptosis, demonstrating that autophagy exerted a protective effect on Res-induced apoptosis in 786-O cells. To the best of our knowledge, only one study (38) has reported the role of Res-induced autophagy in RCC, demonstrating that Res induces autophagy via the AMPK-mTOR signaling pathway and that autophagy, in turn, promotes apoptosis. This difference may be attributed to the different cell lines used. Furthermore, the previous study only detected the expression levels of autophagy-associated proteins and genes to ascertain their effect on Res-mediated apoptosis. In the absence of autophagic flux studies, their evidence remains unconvincing.

Overall, ROS was involved in the process of Res-induced apoptosis in 786-O cells. On the one hand, ROS damaged mitochondria and activated caspase to execute apoptosis. On the other hand, it induced autophagy through JNK, and autophagy suppressed apoptosis. Therefore, a combination of Res and autophagy inhibitor could enhance the inhibitory effect of Res on RCC.

Acknowledgements

Not applicable.

Funding

The present study was funded by the Natural Science Foundation of Jiangsu Province (grant no. BK20151180), the Applied Basic Research of Changzhou City (grant no. CJ20159014) and the Major Science and Technology Project of Changzhou Health Bureau (grant no. ZD201405).

Availability of data and materials

The datasets used and/or analysed in the present study are available from the corresponding author upon reasonable request.

Authors' contributions

HY and MF interpreted the data and drafted the initial manuscript. XH designed the experiments and revised the initial manuscript and HY performed the experiments. All authors read and approved the final manuscript

Ethics approval and consent to participate

Not applicable.

Patient consent for publication

Not applicable.

Competing interests

The authors declare that they have no competing interests.

References

1. Simard EP, Ward EM, Siegel R, Jemal A: Cancers with increasing incidence trends in the United States: 1999 through 2008. *CA Cancer J Clin* 62: 118-128, 2012.
2. Znaor A, Lortet-Tieulent J, Laversanne M, Jemal A and Bray F: International variations and trends in renal cell carcinoma incidence and mortality. *Eur Urol* 67: 519-530, 2015.
3. Motzer RJ, Agarwal N, Beard C, Bhayani S, Bolger GB, Carducci MA, Chang SS, Choueiri TK, Hancock SL, Hudes GR, *et al*: Kidney cancer. *J Natl Compr Canc Netw* 9: 960-977, 2011.
4. Novelle MG, Wahl D, Diéguez C, Bernier M and de Cabo R: Resveratrol supplementation: Where are we now and where should we go? *Ageing Res Rev* 21: 1-15, 2015.
5. Jang M, Cai L, Udeani GO, Slowing KV, Thomas CF, Beecher CW, Fong HH, Farnsworth NR, Kinghorn AD, Mehta RG, *et al*: Cancer chemopreventive activity of resveratrol, a natural product derived from grapes. *Science* 275: 218-220, 1997.
6. Carter LG, D'Orazio JA and Pearson KJ: Resveratrol and cancer: Focus on in vivo evidence. *Endocr Relat Cancer* 21: R209-R225, 2014.
7. Iliopoulos O, Kibel A, Gray S and Kaelin WG Jr: Tumour suppression by the human von Hippel-Lindau gene product. *Nat Med* 1: 822-826, 1995.
8. Kucejova B, Peña-Llopis S, Yamasaki T, Sivanand S, Tran TA, Alexander S, Wolff NC, Lotan Y, Xie XJ, Kabbani W, *et al*: Interplay between pVHL and mTORC1 pathways in clear-cell renal cell carcinoma. *Mol Cancer Res* 9: 1255-1265, 2011.
9. Khan MA, Chen HC, Wan XX, Tania M, Xu AH, Chen FZ and Zhang DZ: Regulatory effects of resveratrol on antioxidant enzymes: A mechanism of growth inhibition and apoptosis induction in cancer cells. *Mol Cells* 35: 219-225, 2013.
10. Chen LB: Mitochondrial membrane potential in living cells. *Annu Rev Cell Biol* 4: 155-181, 1988.
11. Dröge W: Free radicals in the physiological control of cell function. *Physiol Rev* 82: 47-95, 2002.
12. Dewaele M, Maes H and Agostinis P: ROS-mediated mechanisms of autophagy stimulation and their relevance in cancer therapy. *Autophagy* 6: 838-854, 2010.
13. Chan LL, Shen D, Wilkinson AR, Patton W, Lai N, Chan E, Kuksin D, Lin B and Qiu J: A novel image-based cytometry method for autophagy detection in living cells. *Autophagy* 8: 1371-1382, 2012.
14. Pajares M, Jiménez-Moreno N, Dias IHK, Debelec B, Vucetic M, Fladmark KE, Basaga H, Ribaric S, Milisav I and Cuadrado A: Redox control of protein degradation. *Redox Biol* 6: 409-420, 2015.
15. Xu J, Wu Y, Lu G, Xie S, Ma Z, Chen Z, Shen HM and Xia D: Importance of ROS-mediated autophagy in determining apoptotic cell death induced by physapubescin B. *Redox Biol* 12: 198-207, 2017.
16. Xie X, Le L, Fan Y, Lv L and Zhang J: Autophagy is induced through the ROS-TP53-DRAM1 pathway in Response to mitochondrial protein synthesis inhibition. *Autophagy* 8: 1071-1084, 2012.
17. Hung AC, Tsai CH, Hou MF, Chang WL, Wang CH, Lee YC, Ko A, Hu SC, Chang FR, Hsieh PW and Yuan SS: The synthetic β -nitrostyrene derivative CYT-Rx20 induces breast cancer cell death and autophagy via ROS-mediated MEK/ERK pathway. *Cancer Lett* 371: 251-261, 2016.
18. Tsao CC and Corn PG: MDM-2 antagonists induce p53-dependent cell cycle arrest but not cell death in renal cancer cell lines. *Cancer Biol Ther* 10: 1315-1325, 2010.
19. Wei Y, Pattingre S, Sinha S, Bassik M and Levine B: JNK1-mediated phosphorylation of Bcl-2 regulates starvation-induced autophagy. *Mol Cell* 30: 678-688, 2008.
20. Mariño G, Niso-Santano M, Baehrecke EH and Kroemer G: Self-consumption: The interplay of autophagy and apoptosis. *Nat Rev Mol Cell Biol* 15: 81-94, 2014.

21. Gurkar AU, Chu K, Raj L, Bouley R, Lee SH, Kim YB, Dunn SE, Mandinova A and Lee SW: Identification of ROCK1 kinase as a critical regulator of Beclin1-mediated autophagy during metabolic stress. *Nat Commun* 4: 2189, 2013.
22. Otera H, Ohsakaya S, Nagaura Z, Ishihara N and Mihara K: Export of mitochondrial AIF in response to proapoptotic stimuli depends on processing at the intermembrane space. *EMBO J* 24: 1375-1386, 2005.
23. Brenner C and Kroemer G: Apoptosis. Mitochondria-the death signal integrators. *Science* 289: 1150-1151, 2000.
24. Muqbil I, Beck FW, Bao B, Sarkar FH, Mohammad RM, Hadi SM and Azmi AS: Old wine in a new bottle: The warburg effect and anticancer mechanisms of resveratrol. *Curr Pharm Des* 18: 1645-1654, 2012.
25. Miki H, Uehara N, Kimura A, Sasaki T, Yuri T, Yoshizawa K and Tsubura A: Resveratrol induces apoptosis via ROS-triggered autophagy in human colon cancer cells. *Int J Oncol* 40: 1020-1028, 2012.
26. Gu S, Chen C, Jiang X and Zhang Z: ROS-mediated endoplasmic reticulum stress and mitochondrial dysfunction underlie apoptosis induced by resveratrol and arsenic trioxide in A549 cells. *Chem Biol Interact* 245: 100-109, 2016.
27. Kim C, Baek SH, Um JY, Shim BS and Ahn KS: Resveratrol attenuates constitutive STAT3 and STAT5 activation through induction of PTP ϵ and SHP-2 tyrosine phosphatases and potentiates sorafenib-induced apoptosis in renal cell carcinoma. *BMC Nephrol* 17: 19, 2016.
28. Moriyama M, Moriyama H, Uda J, Kubo H, Nakajima Y, Goto A, Morita T and Hayakawa T: BNIP3 upregulation via stimulation of ERK and JNK activity is required for the protection of keratinocytes from UVB-induced apoptosis. *Cell Death Dis* 8: e2576, 2017.
29. Wang X, Luo F and Zhao H: Paraquat-induced reactive oxygen species inhibit neutrophil apoptosis via a p38 MAPK/NF- κ B-IL-6/TNF- α positive-feedback circuit. *PLoS One* 9: e93837, 2014.
30. Kumar B, Iqbal MA, Singh RK and Bamezai RN: Resveratrol inhibits TIGAR to promote ROS induced apoptosis and autophagy. *Biochimie* 118: 26-35, 2015.
31. Yan HW, Hu WX, Zhang JY, Wang Y, Xia K, Peng MY and Liu J: Resveratrol induces human K562 cell apoptosis, erythroid differentiation, and autophagy. *Tumour Biol* 35: 5381-5388, 2014.
32. Alayev A, Sun Y, Snyder RB, Berger SM, Yu JJ and Holz MK: Resveratrol prevents rapamycin-induced upregulation of autophagy and selectively induces apoptosis in TSC2-deficient cells. *Cell Cycle* 13: 371-382, 2014.
33. Alayev A, Berger SM, Kramer MY, Schwartz NS and Holz MK: The combination of rapamycin and resveratrol blocks autophagy and induces apoptosis in breast cancer cells. *J Cell Biochem* 116: 450-457, 2015.
34. Simon HU, Friis R, Tait SW and Ryan KM: Retrograde signaling from autophagy modulates stress responses. *Sci Signal* 10: pii: eaag2791, 2017.
35. de la Cruz-Morcillo MA, Valero ML, Callejas-Valera JL, Arias-González L, Melgar-Rojas P, Galán-Moya EM, García-Gil E, García-Cano J and Sánchez-Prieto R: P38MAPK is a major determinant of the balance between apoptosis and autophagy triggered by 5-fluorouracil: Implication in resistance. *Oncogene* 31: 1073-1085, 2012.
36. Masoud GN and Li W: HIF-1 α pathway: Role, regulation and intervention for cancer therapy. *Acta Pharm Sin B* 5: 378-389, 2015.
37. Kaminskyy VO and Zhivotovsky B: Free radicals in cross talk between autophagy and apoptosis. *Antioxid Redox Signal* 21: 86-102, 2014.
38. Liu Q, Fang Q, Ji S, Han Z, Cheng W and Zhang H: Resveratrol-mediated apoptosis in renal cell carcinoma via the p53/AMP-activated protein kinase/mammalian target of rapamycin autophagy signaling pathway. *Mol Med Rep* 17: 502-508, 2018.



This work is licensed under a Creative Commons Attribution-NonCommercial-NoDerivatives 4.0 International (CC BY-NC-ND 4.0) License.